Chemosphere 77 (2009) 895–901

Contents lists available at ScienceDirect

Chemosphere

journal homepage: www.elsevier.com/locate/chemosphere

# Trichlorfon-induced apoptosis in hepatocyte primary cultures of *Carassius auratus gibelio*

Wei-Na Xu [a,b], Wen-Bin Liu [a,b,*], Zhao-Pu Liu [c]

[a] College of Animal Science and Technology, Nanjing Agricultural University, Nanjing 210095, China
[b] College of Fisheries, Nanjing Agricultural University, Wuxi 214081, China
[c] College of Resources and Environmental Sciences, Nanjing Agricultural University, Nanjing 210095, China

ARTICLE INFO

*Article history:*
Received 6 May 2009
Received in revised form 21 August 2009
Accepted 23 August 2009
Available online 22 September 2009

*Keywords:*
Apoptosis
*Carassius auratus gibelio* hepatocytes
Primary culture
Trichlorfon

ABSTRACT

Trichlorfon, an organophosphorus pesticide, can disrupt metabolism, reproduction and immune functions of some aquatic animals. In the present study, the effect of trichlorfon on apoptosis and the underlying apoptotic mechanism were investigated in primary cultures of *Carassius auratus gibelio* hepatocytes. Analyses of cultures exposed to 0, 0.01, 0.1, and 1.0 mg $L^{-1}$ trichlorfon concentrations for 24 h indicated that trichlorfon induced apoptosis and caused nuclear shrinkage, cell membrane rupture, cytoskeletal collapse, loss of cytoplasm, mitochondria vacuolization, and apoptotic body formation, as well as lipid droplet accumulation. Trichlorfon increased intracellular reactive oxygen species and malondialdehyde concentrations and caused cytochrome c release from mitochondria into the cytoplasm, leading to caspase-3 activation. These findings contributed to a better understanding of the mechanisms underlying trichlorfon-induced apoptosis via activation of mitochondrial pathways while clearly indicating that trichlorfon-induced cell death was via apoptosis accompanied by mitochondrial cytochrome c release and consequent caspase-3 activation.



## 1. Introduction

Trichlorfon [O,O-dimethyl-(2,2,2-trichloro-1-hydroxyethyl)-phosphonate], an organophosphorus pesticide (OP), is currently used in aquaculture to control ectoparasites owing to its relatively low bioaccumulation and short-term persistence (Lopes et al., 2006). Trichlorfon dosage to eradicate ectoparasites varies from 0.1 to 1 mg $L^{-1}$ in ponds (Chang et al., 2006), but excessive amounts are often applied in fishery and agricultural farm management, resulting in trichlorfon-polluted waters. The pesticide's residues in the water has raised concerns over trichlorfon's potential to cause health effects in non-targeted species such as fish, crabs, and shrimp (Hong et al., 2003; Soumis et al., 2003; Guimara et al., 2006). Trichlorfon exerts its toxic effects in animals mainly by the inhibition of acetylcholinesterase at skeletal muscle synaptic and neuromuscular junctions, and is also capable of altering an organism's antioxidant defense system, inducing oxidative stress both *in vitro* (Feng et al., 2007; Hong et al., 2007) and *in vivo* (Chang et al., 2006).

Oxidative stress seems to be the central element in the regulation of the apoptotic pathway triggered by environmental stressors (Barzilai and Yamamoto, 2004; Shi et al., 2004; Ott et al., 2007). Yu et al. (2008) demonstrated OP insecticide chlorpyrifos-induced cell apoptosis in mouse retina via oxidative stress. Apoptosis may be induced either by the extrinsic pathway involving cell surface death receptors or by the intrinsic pathway induced by intracellular stimuli that transmit a signal to mitochondria (Rea-Boutrois et al., 2008). Oxidative stress-induced apoptosis has been largely associated with activation of apoptotic intrinsic pathways at the mitochondrial level (Francoa et al., 2009). It has been reported that OPs, e.g., paraoxon (POX), dichlorvos, and chlorpyrifos, induced cell apoptosis via activation of mitochondrial pathways, including caspase-3 activation and the release of cytochrome c into the cytosol (Saleh et al., 2003; Li et al., 2007; Saulsbury et al., 2008, 2009). Despite previous investigations into OP insecticide-induced apoptosis, the biological action and molecular mechanism of trichlorfon-induced apoptosis are still not clear.

The aim of this study is to broaden the understanding of the mechanisms of trichlorfon-induced apoptosis *in vitro* by investigation of trichlorfon cytotoxicity in primary hepatocyte cultures of *Carassius auratus gibelio*. The effects of different trichlorfon concentrations are assessed in terms of changes in reactive oxygen species (ROS) and malondialdehyde (MDA) concentrations, cell viability, apoptotic ratios, release of cytochrome c, and caspase-3 activity. Additionally, hepatocyte ultrastructural changes are observed by transmission electron microscope (TEM). The liver, an important site for biotransformation and bioaccumulation of xenobiotic

* Corresponding author. Address: College of Animal Science and Technology, Nanjing Agricultural University, Nanjing 210095, China. Tel.: +86 25 84395382/13901590642; fax: +86 25 84395382.
*E-mail address:* wbliu@njau.edu.cn (W.-B. Liu).

0045-6535/$ - see front matter © 2009 Elsevier Ltd. All rights reserved.
doi:10.1016/j.chemosphere.2009.08.043

substances (Filipak-Neto et al., 2007), is intensively studied as a target organ for toxicology and risk assessment. Cultured primary hepatocytes of *C. auratus gibelio* provide rapid, easy, and sensitive approaches to ecotoxicological studies of freshwater fish, e.g., investigations of enzyme variability and cytotoxic metabolism, which may help in gaining valuable information for drug utilization in aquaculture.

## 2. Materials and methods

### 2.1. Materials

Trichlorfon (99.9% purity) was purchased from Sigma Chemical Co. (St. Louis, MO, USA). Dulbecco modified Eagle medium (DMEM): F-12 (1:1) medium, fetal bovine serum, phosphate buffered saline without $Ca^{2+}$ and $Mg^{2+}$ (PBS), 0.25% trypsin–ethylene diamine tetraacetic acid (trypsin–EDTA), antibiotics (10 000 IU $mL^{-1}$ penicillin G sodium, 10 000 IU $mL^{-1}$ streptomycin), and trypan-blue were obtained from GIBCO BRL (Grand Island, New York, USA). Polystyrene Corning 25 mL cell culture flasks, 6-well plates, and 96-well plates were purchased from Corning, Inc. (Corning, New York, USA).

### 2.2. Hepatocyte primary culture

Hepatocytes culture was carried out as previously described (Arat et al., 2002). Briefly, fish were sacrificed and disinfected with 75% alcohol, liver samples rapidly isolated from the body and washed several times in ice-cold PBS containing antibiotic (100 IU $mL^{-1}$ penicillin G sodium and 100 IU $mL^{-1}$ streptomycin). After removal of PBS by sterile pipette, the samples were cut into small pieces (~1 mm) with a scalpel, placed into culture flasks and routinely cultured in fresh DMEM/F12 medium in the presence of 15% serum and 100 IU $mL^{-1}$ of antibiotic (as above) at 25 °C in an incubator with 5% $CO_2$, with the medium replaced every 3 d. After 1 week, cells were observed growing out of the explants and the explants removed. Upon reaching confluency, cells were harvested by trypsinization (0.25% trypsin–EDTA), suspended at a density of $1 \times 10^6$ cells $mL^{-1}$, and counted using trypan-blue (0.4%, Wang et al., 2008) with inverted microscope (TE 2000 Microscope, Nikon, Japan) to confirm that cell viability exceeded 90% for subsequent experimentation.

### 2.3. Cell treatment

Cultured cell suspensions were seeded onto 6-well plates, incubated at 25 °C, and medium replaced every 3 d until 80–90% confluent, at which time they were cultured in medium containing a range of trichlorfon concentrations (0, 0.01, 0.1, and 1.0 mg $L^{-1}$) for 24 h at 25 °C. The trichlorfon half-life time in water was 2.5 d and the 95% dissipation time of the chemical was 10.2 d (Lopes et al., 2006). After exposure, cells were harvested by trypsinization (0.25% trypsin–EDTA) at room temperature and suspended at a density of $1 \times 10^7$ cells $mL^{-1}$ for cellular biochemical and apoptotic assays.

### 2.4. Cell proliferation assay

Hepatocyte proliferation was assayed using a Cell Counting Kit-8 (CCK-8, Dojindo Laboratories, Kumamoto, Japan) following the manufacturer's protocol. This assay is an enzymatic test based on the determination of mitochondrial dehydrogenase enzyme activities (Yoshimura et al., 2002). Briefly, 100 μL of primary cell culture suspension ($5–10 \times 10^4$ cells $mL^{-1}$) was added to each well of a 96-well plate, incubated in 5% $CO_2$ at 25 °C for 48 h, and then treated with trichlorfon at 0, 0.01, 0.1, 1 mg $L^{-1}$ for 24 h. 10 μL of CCK-8 solution was then added to each well, incubated for a further 4 h, and the OD value read at 450 nm with an enzyme-liked immunosorbent assay (ELISA) reader (Multiskan Spectrum, Thermo Scientific, USA).

### 2.5. Intracellular ROS assay

Accumulation of intracellular ROS was assayed by the fluorescence emission of 2′,7′-dichlorofluorescin diacetate (DCF-DA, Hempel et al., 1999). Briefly, 500 μL of trichlorfon-treated hepatocytes suspension ($1 \times 10^7$ cells $mL^{-1}$) were incubated in PBS buffer with 10 μmol $L^{-1}$ DCF-DA in the dark for 1 h at 25 °C and the fluorescence intensity determined using a fluorescence microplate reader (Infinite M200, TECAN, Switzerland) with excitation at 488 nm and emission at 525 nm (Roos et al., 2009).

### 2.6. Intracellular MDA concentration measurement

After trichlorfon exposure, hepatocytes suspensions ($1 \times 10^7$ cells $mL^{-1}$) were disrupted with a glass tissue grinder, centrifuged at 800*g* at 4 °C for 10 min, and the supernatant collected. The MDA concentration was determined by the method of Ohkawa et al. (1979) with a MDA Detection kit from Nanjing Jian Cheng Biology Company (Nanjing, China) and expressed as nmol mg $protein^{-1}$. Total cellular proteins were quantified by the classical Bradford method with Coomassie Brilliant Blue G-250 (Bradford, 1976).

### 2.7. Apoptosis detection

#### 2.7.1. Annexin V-FITC/PI assay

Apoptotic and necrotic were quantified by measuring externalized phosphatidylserine (PS) assessed by Annexin V-FITC (Dong et al., 2005) and by propidium iodide (PI) uptake (Li et al., 1999) using an Annexin V-FITC/PI Apoptosis Detection Kit (Nanjing Keygen Biotech. Co., Ltd.). Briefly, after trichlorfon exposure, 250 μL of cell suspension ($1 \times 10^7$ cells $mL^{-1}$) were stained by mixing with 2 μL each of Annexin V-FITC and PI and incubation at room temperature in the dark for 15 min and then the apoptotic cells populations analyzed immediately using a FACScan flow cytometer (Becton Dickinson, San Jose, CA) with excitation at 488 nm and emission at 530 nm (FITC) and 610 (PI).

#### 2.7.2. Nuclear morphological analysis

Nuclear morphology analysis was performed using the fluorescent probes acridine orange (AO) and ethidium bromide (EB) (Kasibhatla et al., 1998) and a cell apoptosis AO/EB detection kit (Nanjing Keygen Biotech. Co., Ltd.). After trichlorfon exposure, cultured medium was removed, cells washed twice with PBS, stained with both AO and EB for 5 min in the dark, and washed twice with warm PBS. Cell nuclear morphology was observed under a camera-equipped fluorescence light microscope (Eclipse 90i Microscope, Nikon, Japan) with an excitation wave length of 495 nm and emission at 515 nm (AO) and 600 nm (EB).

#### 2.7.3. Hepatocyte ultrastructure observation

Changes in hepatocyte ultrastructure were confirmed by examination of cell organelles by TEM using a method of Carlson et al. (2000). Briefly, after exposure, cell suspensions ($1 \times 10^7$ cells $mL^{-1}$) were centrifuged, the medium discarded, the cells fixed with 0.25% glutaraldehyde in PBS (pH 7.2) at 25 °C for 4 h, washed in cacodylate buffer, post-fixed with 1% $OsO_4$, dehydrated in a graded series of ethanol solutions, infiltrated by propylene oxide, and finally embedded in epon. Ultrathin sections of the resulting sample were counterstained with 4% uranyl acetate, as well as lead citrate, and observed

using H-7650 Transmission Electron Microscope (Hitachi High-Technologies Co., Japan).

### 2.8. ELISA analysis of cytochrome c

Cytochrome c was analyzed in mitochondrial and cytosolic fractions by isolation of mitochondrial and cytosolic proteins using the mitochondria/cytosol Fractionation Kit (Hanzel and Verstraeten, 2009; Beyotime Inst. Biotech, Peking, China). Briefly, after exposure, hepatocytes ($1 \times 10^7$ cells $mL^{-1}$) were harvested and centrifuged at 800*g* at 4 °C for 10 min, the pellets combined with 0.2 mL of 20 mM N-2-hydroxyethylpiperazine-N′-2′-ethanesulfonic acid (HEPES) buffer containing protease inhibitor (phenylmethanesulfonyl fluoride, 1 mmol $L^{-1}$), and disrupted using a glass tissue grinder. Homogenates were centrifuged at 800*g* at 4 °C for 10 min, the resulting supernatants transferred to 0.5 mL conical tubes, and further centrifuged at 10 000*g* at 4 °C for 20 min. The final supernatants and pellets, containing the cytosolic and mitochondrial fractions, respectively, were analyzed for protein content (Bradford, 1976) and cytochrome c concentrations were determined using an enzyme-linked immunosorbent kit (ADL Co-Lab, USA), according to the manufacturer's protocol, with the optical density (OD) of each well determined using an ELISA reader at 450 nm and a cytochrome c calibration curve.

### 2.9. Caspase-3 measurement

Caspase-3 activity was measured using a caspase-3 cellular activity assay kit (Nanjing Keygen Biotech. Co., Ltd.) according to the manufacturer's protocol. Briefly, after trichlorfon exposure, cells ($1 \times 10^7$ cells $mL^{-1}$) were lysed in ice-cold buffer (50 mM HEPES, 5 mM DL-dithiothreitol (DL-DTT), 0.1 mM EDTA, and 0.1% 3-[(3-cholamidopropyl) dimethylammonio] propanesulfonic acid (CHAPS) for 20 min, and the lysates clarified by centrifugation at 10 000*g* at 4 °C for 10 min. About 50 μL of supernatant was mixed with 100 μL reaction buffer and 5 μL of caspase-3 substrate, incubated at 25 °C in the dark for 4 h, and the OD measured with an ELISA reader at 405 nm (Han et al., 2007). The caspase-3activity was calculated as OD (test)/OD (control) (test and control, absorbance of cells with and without trichlorfon treatment, respectively).

### 2.10. Statistical analysis

Data were expressed as means ± standard error and, after testing homogeneity of variance, statistical differences between treatment and control groups determined by a single-factor one-way ANOVA followed by LSD multiple comparison tests when variances were homogeneous. When there was variance heterogeneity, multiple pairwise comparisons were made by Tamhane's T2 test. Values were calculated using SPSS 16.0 software. For all tests, the level of significance was set at $p < 0.05$.

## 3. Results

### 3.1. Trichlorfon effects on oxidative stress in hepatocytes

After exposure to 0.01, 0.1, and 1 mg $L^{-1}$ trichlorfon, cultured hepatocyte ROS concentrations were significantly ($p < 0.05$) increased compared to untreated control cells (Fig. 1A) and ROS concentrations in the 1 mg $L^{-1}$ trichlorfon treatment were significantly higher ($p < 0.05$) than at 0.01 and 0.1 mg $L^{-1}$. The intracellular MDA concentration was also examined to determine if increased production of ROS may have played a role in trichlorfon-induced oxidative toxicity and similar results were obtained after treatments with trichlorfon for 24 h. These results suggested

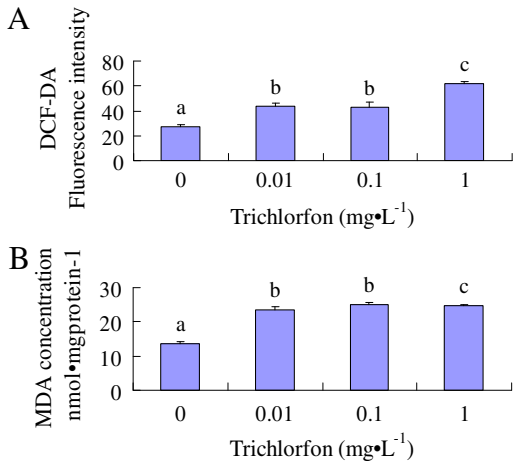


**Fig. 1.** Trichlorfon effects on *C. auratus gibelio* hepatocyte ROS and MDA concentrations. Hepatocytes incubated with 0, 0.01, 0.1, and 1 mg $L^{-1}$ trichlorfon for 24 h: (A) trichlorfon effects on intercellular ROS concentrations; (B) trichlorfon effects on intercellular MDA concentrations; results mean ± SEM of six experiments; bars, different letters denote results significantly different from control ($p < 0.05$), same letters denote results not different ($p > 0.05$).

that the trichlorfon-induced generation of ROS played a significant role in trichlorfon-induced MDA in these hepatocytes (Fig. 1B).

### 3.2. Trichlorfon effects on hepatocyte viability, apoptosis, and necrosis

Increasing concentrations of trichlorfon resulted in a dose-dependent decrease in cell viability as measured by the CCK-8 cell proliferation assay (Fig. 2). Generally, as the trichlorfon concentration increased, cell viability decreased ($p < 0.05$); hepatocyte viability treated with 0.01, 0.1, and 1 mg $L^{-1}$ trichlorfon were 79.21%, 61.66%, and 52.75% of the control value, respectively, and significantly decreased ($p < 0.05$) compared to control cells. Interestingly, there was no significant difference in viability between 0.1 and 1 mg $L^{-1}$ trichlorfon at 24 h ($p > 0.05$).

The result of flow cytometry analysis revealed that trichlorfon-induced apoptosis in hepatocytes in a dose-dependent manner with the proportion of apoptotic cells significantly increased ($p < 0.05$) in 0.01, 0.1, and 1 mg $L^{-1}$ trichlorfon groups compared with the control (Fig. 3A). Here, also, there was no significant difference between cells treated with 0.1 and 1 mg $L^{-1}$ trichlorfon at 24 h ($p > 0.05$). The proportion of necrotic cells in the presence of trichlorfon was similar to the control cells (Fig. 3).

### 3.3. Trichlorfon effects on hepatocyte nuclear morphology and ultrastructure

AO/EB double-staining revealed significant changes in the nuclear morphology of trichlorfon-treated cells compared to the controls. Cells in control fluoresced brightly, and were proportional

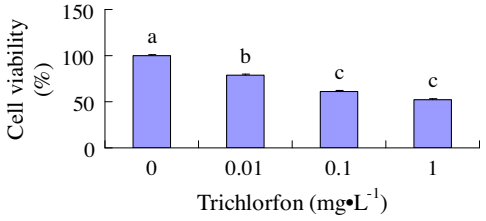


**Fig. 2.** Trichlorfon effects on *C. auratus gibelio* hepatocyte viability. Cell viability assayed using Cell Counting Kit-8; hepatocytes incubated with 0, 0.01, 0.1, and 1 mg $L^{-1}$ trichlorfon; data from at least six experiments; results, mean ± SEM; bars, different letters denote results significantly different from control ($p < 0.05$), same letters denote results not different ($p > 0.05$).

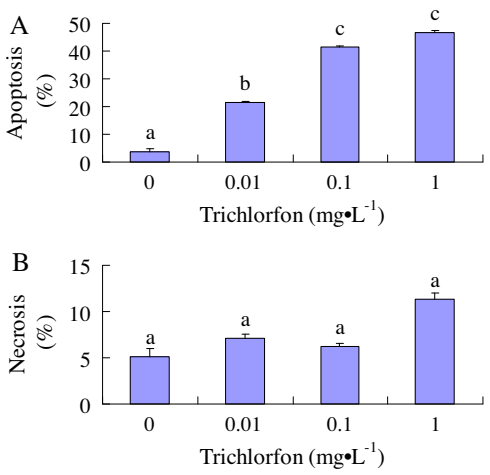


**Fig. 3.** Trichlorfon effects on *C. auratus gibelio* hepatocyte apoptosis and necrosis using Annexin V-FITC/PI assay. Hepatocytes incubated with 0, 0.01, 0.1, and 1 mg $L^{-1}$ trichlorfon: (A) trichlorfon effects on apoptosis; (B) trichlorfon effects on cell necrosis; results, mean ± SEM of six experiments; bars, different letters denote results significantly different from control ($p < 0.05$), same letters denote results not different ($p > 0.05$).

and well distributed and cells were integrity and uniformity (Fig. 4A). In contrast, at 0.01 mg $L^{-1}$ trichlorfon exposure, the cell growth condition is not good. Some cells were piled up in together, presented irregular shape. Most nuclei were stained orange and some retained a regular shape while others were irregularly shaped with signs of pycnosis (Fig. 4B). At 0.1 mg $L^{-1}$ trichlorfon, cell membranes were ruptured, and there was cytoskeletal collapse, nucleus shrinkage, and orange luminescent apoptotic body formation (Fig. 4C). At 1.0 mg $L^{-1}$ trichlorfon, there was no cell integrity and orange fluorescing particles were observed (Fig. 4D).

Examination of the hepatocytes by TEM showed that normal hepatocytes were polyhedral, with a spherical nucleus. In a typical cell, the nuclei, round and big, was found in the center of the cell and the cytomembranes intact. Rough endoplasmic reticulum (RER) and mitochondria were abundant in the cytoplasm and the RER was continuous with the external nuclear membrane and concentrated in the perinuclear region (Fig. 5A). On exposure to 0.01 mg $L^{-1}$ trichlorfon, large numbers of lipid droplets were present, mitochondria vacuolated, cristae lost, and broken mitochondrial membranes observed (Fig. 5B). With 0.1 mg $L^{-1}$ trichlorfon treatment, broken mitochondrial membranes, vacuolization of mitochondria, loss of cytoplasm, and pycnotic nuclei were observed (Fig. 5C). At 1 mg $L^{-1}$, organelles were covered with highly polymorphic lipid droplets and loss of cytoplasm was observed (Fig. 5D).

### 3.4. Trichlorfon effects on cytochrome c levels

Trichlorfon induced a dose-dependent increase in cytochrome c concentrations in the cytosol and decrease its concentrations in mitochondria (Fig. 6). Even at the lowest concentration, trichlorfon significantly ($p < 0.05$) induced cytochrome c release from mitochondria into cytoplasm.

### 3.5. Trichlorfon effects on caspase-3 activities

Caspase-3 plays a critical role in the mitochondrial apoptotic signaling pathway. The present results showed that exposure to 0.01, 0.1, and 1 mg $L^{-1}$ trichlorfon caused significant ($p < 0.05$) increases in caspase-3 activity compared to untreated control cells

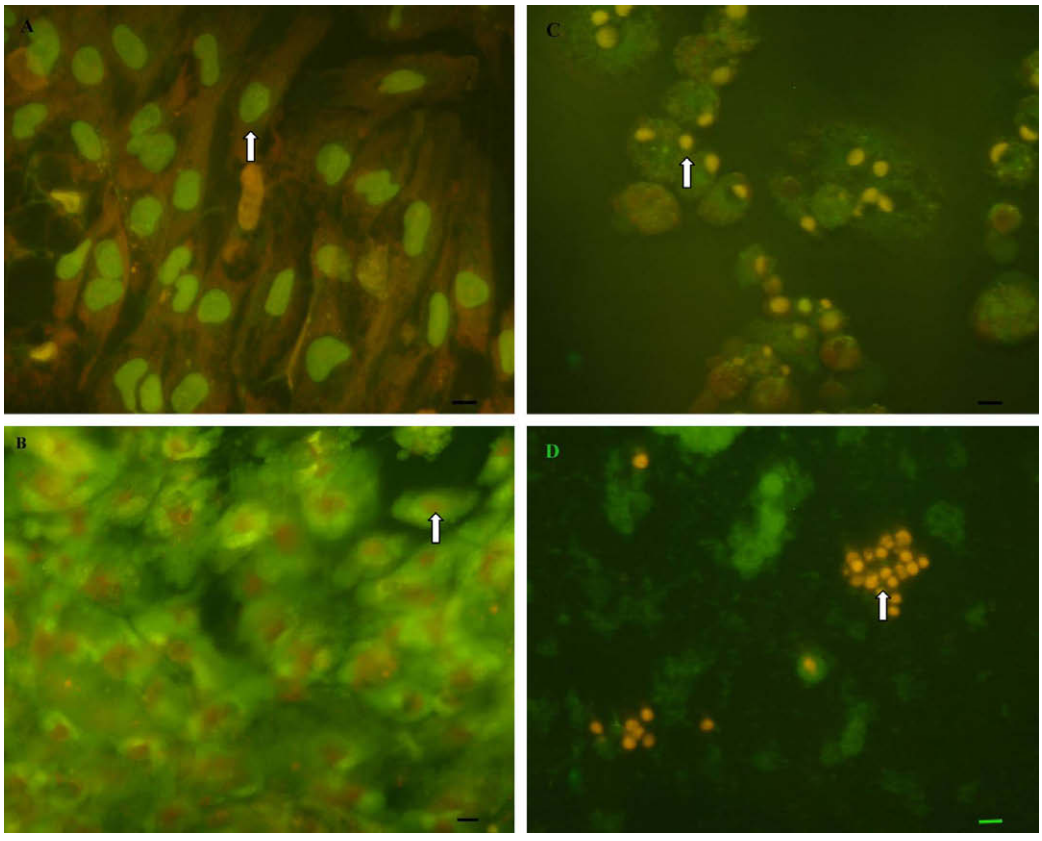


**Fig. 4.** Trichlorfon effects on *C. auratus gibelio* hepatocytes nuclear morphology. Observations performed using AO/EB fluorescent staining and fluorescent microscopy; arrows indicate apoptotic cells: (A) control cells, nucleus (↑), 400×, bar = 100 μm; (B) 0.01 mg $L^{-1}$ trichlorfon treatment, nucleus (↑), 400×, bar = 50 μm; (C) 0.1 mg $L^{-1}$ trichlorfon treatment, apoptotic body formation (↑), 400×, bar = 50 μm; and (D) 1.0 mg $L^{-1}$ trichlorfon treatment, orange fluorescing particles (↑), 400×, bar = 50 μm.

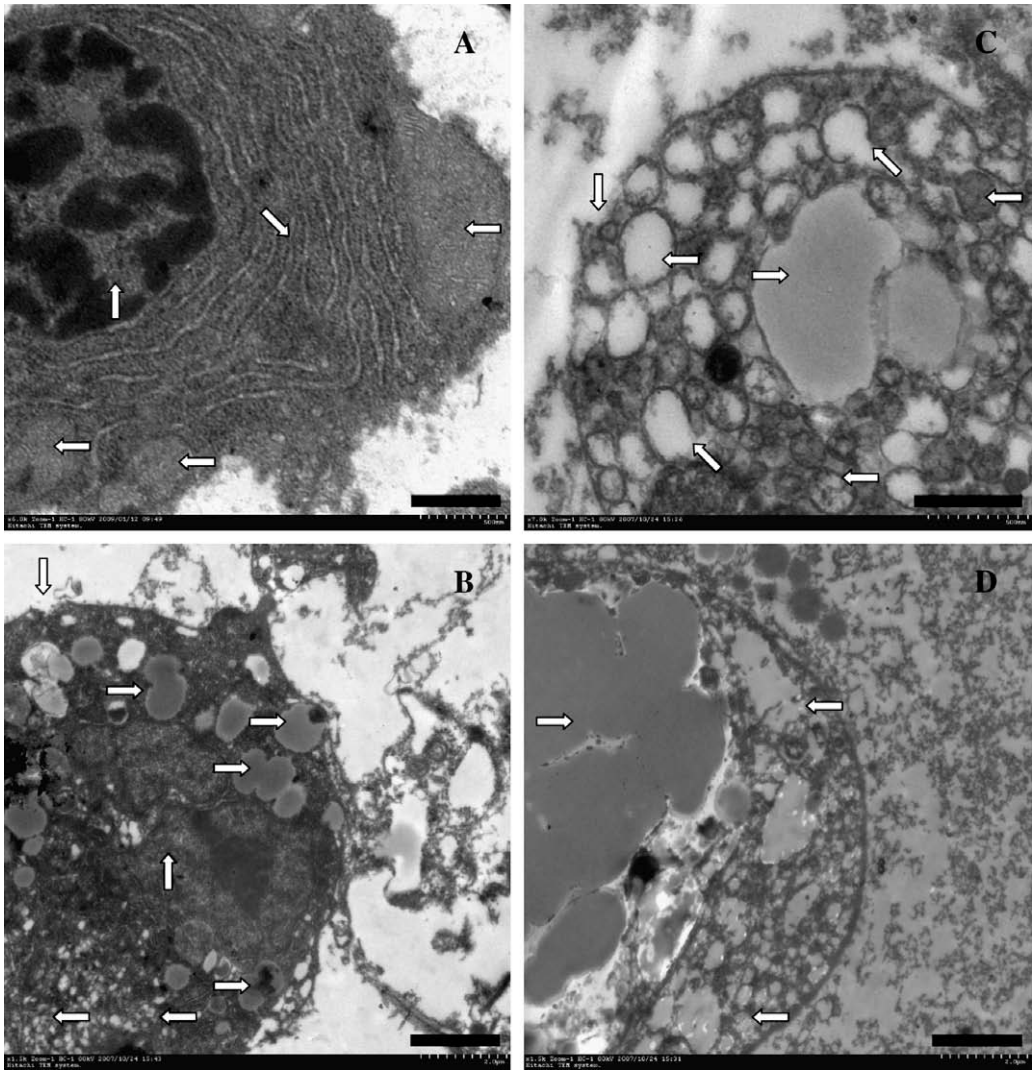


**Fig. 5.** TEM images of *C. auratus gibelio* hepatocyte cell structural organization following trichlorfon treatment: (A) control cells, nucleus (↑), mitochondria (←), and RER (↘) in cytoplasm, bar = 500 nm; (B) 0.01 mg $L^{-1}$ trichlorfon treatment, nucleus (↑), dilatation of mitochondria (←), large numbers of lipid droplets (→), disrupted cytomembrane (↓), bar = 2.0 μm; (C) 0.1 mg $L^{-1}$ trichlorfon treatment, broken mitochondrial membranes (↖), mitochondrial vacuolization (←), disrupted cytomembrane (↓), bar = 500 nm; and (D) 1 mg $L^{-1}$ trichlorfon treatment, lipid droplets (→), vacuolization of mitochondria (←), bar = 2 μm.

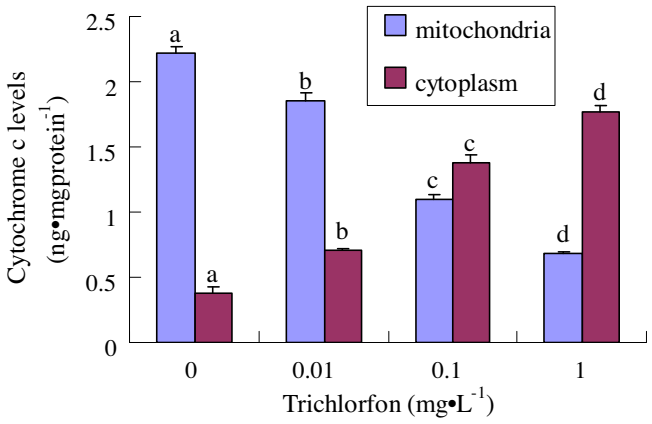


**Fig. 6.** Trichlorfon effects on *C. auratus gibelio* hepatocytic mitochondrial and cytosolic cytochrome c concentrations from ELISA analyses. Hepatocytes incubated with 0, 0.01, 0.1, and 1 mg $L^{-1}$ trichlorfon; results, mean ± SEM of six experiments; bars, different letters denote results significantly different from control ($p < 0.05$), same letters denote results not different ($p > 0.05$).

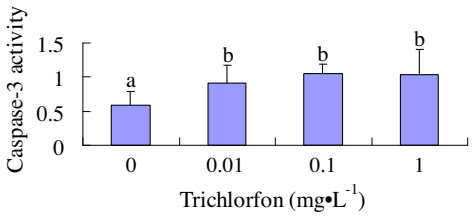


**Fig. 7.** Trichlorfon effects on *C. auratus gibelio* hepatocyte caspase-3 activity. Hepatocytes incubated with 0, 0.01, 0.1, and 1 mg $L^{-1}$ trichlorfon; caspase-3 activity assayed by caspase-3 colorimetric assay kit; results, mean ± SEM of six experiments; bars, different letters denote results significantly different from control ($p < 0.05$), same letters denote results not different ($p > 0.05$).

(Fig. 7). No significant differences were found between 0.01, 0.1, and 1 mg $L^{-1}$ trichlorfon ($p > 0.05$).

## 4. Discussion

In the present study, primary *C. auratus gibelio* hepatocytes cultures were employed to demonstrate trichlorfon cytotoxicity to

hepatocytes. The proportions of viable cells obtained from CCK-8 analysis declined as trichlorfon concentration increased, while the proportion of necrotic cells showed negligible differences among all groups. The question remained as to how trichlorfon induced cell death.

It is well-known that apoptosis is an important and controlled form of cell death that occurs under a variety of physiological and pathological conditions (Aragane et al., 1998; Han et al., 2007). It has been shown that environmental stressors (metals, particulate matter, and pesticides) can induce apoptotic cell death (Ayed-Boussema et al., 2008; Gong et al., 2009; Hanzel and Verstraeten, 2009; Kobayashia et al., 2009). Thus, possible trichlorfon-induced apoptosis was investigated here and the results demonstrated that trichlorfon led to increased ratio of apoptotic cells. However, the question arose as to which pathway trichlorfon induced hepatocyte apoptosis.

Apoptosis may be induced via the extrinsic pathway by the activation of death receptors or intrinsic pathway by intracellular stimuli that transmit a signal to the mitochondria. In both pathways, the result is activation of the executioner caspase-3, a cysteine protease that plays an essential role in apoptosis by mediating a subsequent lethal chain of events (Porter and Janicke, 1999; Brenner and Kroemer, 2000). Caspase-3 activation can be used as a marker of apoptosis (Han et al., 2007). In earlier studies, the OPs, chlorpyrifos and POX have been shown to induce apoptosis in immune and neural cells by activation of intracellular caspase-3 (Carlson et al., 2000; Saleh et al., 2003; Nakadai et al., 2006; Li et al., 2007). Activation of caspase-3 is associated with morphological and structural changes characteristic of apoptosis. In this study of hepatocytes, morphological examination showed that trichlorfon caused nuclear morphological and ultrastructure changes, including cell membrane rupture, cytoskeletal collapse, nuclear shrinkage, mitochondrial vacuolization, mitochondrial damage, and apoptotic body formation, which were all common apoptotic characteristics. Using AO/EB staining assay, live cells will appear uniformly green; Necrotic cells stain orange, but have a nuclear morphology resembling that of viable cells, with no condensed chromatin; Early apoptotic cells will stain green and contain bright green dots in the nuclei; Late apoptotic cells will stain orange and show condensed and often fragmented nuclei. Nuclear fragmentation using AO/EB staining is an apoptotic hallmark indicative of chromatin condensation and due to an imbalance between the activities of deoxyribonuclease (DNase) and those enzymes responsible for the maintenance of DNA integrity (Hanzel and Verstraeten, 2009). Activated caspase-3 cleaves inhibitor of caspase-activated DNase (ICAD) in a heterodimeric form consisting of caspase-activated DNAse (CAD) and cleaved ICAD (Susin et al., 2000) and the latter dissociates from CAD, allowing formation of CAD oligomers with DNase activity which then cause internucleosomal DNA fragmentation (Pirnia et al., 2002). Here, the role of caspase-3 in trichlorfon-induced apoptosis was confirmed in this system.

Several signaling pathways have been implicated in the initiation of the caspase-3 cascade. One of the most well defined pathways for pro-caspase-3 activation is the translocation of the respiratory chain protein, cytochrome c, from mitochondria to the cytosol (Bossy-Wetzel et al., 1998). The disruption of the mitochondrial membrane potential allows cytochrome c leakage into the cytoplasm (Chipuk et al., 2006; Garrido et al., 2006) where it binds to apoptotic protease activating factor-1 (APAF-1) together with deoxyadenosine triphosphate (dATP), leading to the recruitment and activation of caspase-9 and subsequent activation of caspase-3 (Li et al., 1997). Here, we investigated a key event in the activation of caspase-3, the release of cytochrome c, and demonstrated that trichlorfon-induced apoptosis in primary hepatocytes was accompanied by the increased release of cytochrome c into the cytoplasm with increased trichlorfon concentrations. The mechanism of cytochrome c release from mitochondria is not well understood, but it has been suggested that it may be associated with an increase of cytoplasmic $Ca^{2+}$ (Hong et al., 2003; Bagetta et al., 2004; Yu et al., 2008). It may, however, be induced by ROS interactions with mitochondria (Zhang and Bhavnani, 2005).

In this study, trichlorfon induced hepatocellular oxidative stress by increasing the generation of ROS and MDA concentrations. Oxidative stress appears to be the central element in regulation of apoptotic pathways triggered by environmental stressors (Francoa et al., 2009). Transcription factor p53 is a sensor of cellular stress and a critical activator of the apoptotic intrinsic pathway. This factor may transactivate certain genes which contribute to apoptosis, and other genes which lead to ROS increases (Haupt et al., 2007). When intracellular ROS production exceeds the antioxidant defense capacity of the cell, increased ROS leads to lipid peroxidation and generalized oxidative damage to all mitochondrial components, e g, oxidative mitochondrial DNA (mtDNA) damage, cellular oxidative stress ensues. It was generally accepted that oxidative stress and ROS cause DNA damage, and specific DNA lesions or damage are known to trigger apoptosis (Francoa et al., 2009). Cellular stress-induced apoptosis occurs by a mechanism that involves altering mitochondrial permeability, subsequent cytochrome c release from mitochondria, and formation of the apoptosome, a catalytic multiprotein platform that activates caspase-9 which then cleaves caspase-3, resulting in downstream events involved in cell death (Crow et al., 2004). Thus, from the present results, we deduced that there was a close correlation between the ROS changes and apoptosis observed here.

Interestingly, the lipid accumulation, observed in TEM of hepatocyte ultrastructure that occurred in the trichlorfon-treated groups may have been due to increased lipid peroxidation caused by ROS, which led to mitochondrial vacuolization, structural lesions, and concurrent mitochondrial dysfunction. Mitochondria are often associated with fatty acid-containing oil droplets from which they derive raw materials for oxidation (Karp, 2006), and lipid synthesis and metabolism occurs primarily in mitochondria. Thus, mitochondrial structural lesions may have resulted in early liver steatosis and disorders of lipid metabolism.

## 5. Conclusion

The present findings indicate that trichlorfon induced apoptosis in cultured hepatocytes of *C. auratus gibelio* via the mitochondrial pathway. This pesticide caused increased cellular ROS and MDA concentrations which may impair mitochondrial bioenergetics and physiological functions. Subsequently, the mitochondrial release of cytochrome c into the cytoplasm activated caspase-3 activation, triggering hepatocytes apoptosis. Moreover, mitochondrial structure lesions might be implicated in lipid metabolism disruption. These results contributed to the understanding of the mechanisms underlying trichlorfon toxicity. Further studies are needed to elucidate the precise biological action and the actual molecular mechanism for trichlorfon-induced disorders of lipid metabolism.

## Acknowledgement

The study was supported by The Earmarked Fund for Modern Agro-industry Technology Research System of China (nycytx-49-21).

## References

Aragane, Y., Kulms, D., Metze, D., Wilkes, G., Pöppelmann, B., Luger, T.A., Schwarz, T., 1998. Ultraviolet light induces apoptosis via direct activation of CD95 (Fas/APO-1) independently of its ligand CD95L. J. Cell. Biol. 140 (1), 171–182.

Arat, S., Gibbons, J., Rzucidlo, J., Respess, D.S., Tumlin, M., Stice, S.L., 2002. In vitro development of bovine nuclear transfer embryos from transgenic clonal line of adult and fetal fibroblast cell of the same genotype. Biol. Of. Reprod. 66, 1768–1774.

Ayed-Boussema, I., Bouaziz, C., Rjiba, K., Valenti, K., Laporte, F., Bacha, H., Hassen, W., 2008. The mycotoxin Zearalenone induces apoptosis in human hepatocytes (HepG2) via p53-dependent mitochondrial signaling pathway. Toxicol. in Vitro 22 (7), 1671–1680.

Bagetta, G., Chiappetta, O., Amantea, D., Iannone, M., Rotiroti, D., Costa, A., Nappi, G., Corasaniti, M.T., 2004. Estradiol reduces cytochrome c translocation and minimizes hippocampal damage caused by transient global ischemia in rat. Neurosci. Lett. 368, 87–91.

Barzilai, A., Yamamoto, K., 2004. DNA damage responses to oxidative stress. DNA Repair (Amst). 3, 1109–1115.

Bossy-Wetzel, E., Newmeyer, D.D., Green, D.R., 1998. Mitochondrial cytochrome c release in apoptosis occurs upstream of DEVD-specific caspase activation and independently of mitochondrial transmembrane depolarization. EMBO J. 17, 37–49.

Bradford, M.M., 1976. A rapid and sensitive method for the quantification of microgram quantities of protein utilizing the principle of protein–dye binding. Anal. Biochem. 72, 248–254.

Brenner, C., Kroemer, G., 2000. Apoptosis. Mitochondria—the death signal integrators. Science 289, 1150–1151.

Carlson, K., Jortner, B.S., Ehrich, M., 2000. Organophosphorus compound-induced apoptosis in SH-SY5Y human neuroblastoma cells. Toxicol. Appl. Pharmacol. 168 (2), 102–113.

Chang, C.C., Lee, P.P., Liu, C.H., Cheng, W., 2006. Trichlorfon, an organophosphorus insecticide, depresses the immune responses and resistance to *Lactococcus garvieae* of the giant freshwater prawn *Macrobrachium rosenbergii*. Fish Shellfish. Immunol. 20, 574–585.

Chipuk, J.E., Bouchier-Hayes, L., Green, D.R., 2006. Mitochondrial outer membrane permeabilization during apoptosis: the innocent bystander scenario. Cell. Death. Differ. 13, 1396–1402.

Crow, M.T., Mani, K., Nam, Y.J., Kitsis, R.N., 2004. The mitochondrial death pathway and cardiac myocyte apoptosis. Circ. Res. 95, 957–970.

Dong, C., Li, Q., Lyu, S.C., Krensky, A.M., Clayberger, C., 2005. A novel apoptosis pathway activated by the carboxyl terminus of p21. Blood 105 (3), 1187–1194.

Feng, T., Li, Z.B., Guo, X.Q., Guo, J.P., 2007. Effects of trichlorfon and sodium dodecyl sulfate on antioxidant defense system and acetylcholinesterase of *Tilapia nilotica* in vitro. Pestic. Biochem. Physiol. 92, 107–113.

Filipak-Neto, F., Zanata, S.M., Silva de Assis, H.C., 2007. Use of hepatocytes from *Hoplias malabaricus* to characterize the toxicity of a complex mixture of lipophilic halogenated compounds. Toxicol. in Vitro 21, 706–715.

Francoa, R., Sánchez-Oleab, R., Reyes-Reyesc, E.M., Panayiotidis, M.I., 2009. Environmental toxicity, oxidative stress and apoptosis: Ménage à Trois. Mutat. Res. 674, 3–22.

Garrido, C., Galluzzi, L., Brunet, M., Puig, P.E., Didelot, C., Kroemer, G., 2006. Mechanisms of cytochrome c release from mitochondria. Cell. Death. Differ. 13, 1423–1433.

Gong, Y., Wu, J., Huang, Y., Shen, S., Han, X., 2009. Nonylphenol induces apoptosis in rat testicular sertoli cells via endoplasmic reticulum stress. Toxicol. Lett. 186, 84–95.

Guimara, A.T.B., Silva de Assis, H.C., Boeger, W., 2006. The effect of trichlorfon on acetylcholinesterase activity and histopathology of cultivated fish *Oreochromis niloticus*. Ecotoxicol. Environ. Saf. 68, 57–62.

Han, H., Pan, Q., Zhang, B., Li, Jia., Deng, X., Lian, Z., Li, N., 2007. 4-NQO induces apoptosis via p53-dependent mitochondrial signaling pathway. Toxicology 230, 151–163.

Hanzel, C.E., Verstraeten, S.V., 2009. Tl (I) and Tl (III) activate both mitochondrial and extrinsic pathways of apoptosis in rat pheochromocytoma (PC12) cells. Toxicol. Appl. Pharmacol. 236, 59–70.

Haupt, S., Berger, M., Goldberg, Z., Haupt, Y., 2007. Apoptosis – the p53 network. J. Cell Sci. 116, 4077–4085.

Hempel, S.L., Buettner, G.R.O., Malley, Y.Q., Wessels, D.A., Flaherty, D.M., 1999. Dihydrofluorescein diacetate is superior for detecting intracellular oxidants: comparison with 2′,7′-dichlorodihydrofluorescein diacetate, 5 (and 6)-carboxy-2′,7′-dichloro dihydrofluorescein diacetate, and dihydrorhodamine 123. Free Radical Biol. Med. 27, 146–159.

Hong, M.S., Hong, S.J., Barhoumi, R., Burghardt, R.C., Donnelly, K.C., Wild, J.R., Venkatraj, V., Tiffany-Castiglioni, E., 2003. Neurotoxicity induced in differentiated SK-N-SH-SY5Y human neuroblastoma cells by organophosphorus compounds. Toxicol. Appl. Pharmacol. 186, 110–118.

Hong, X., Qu, J., Chen, J.F., Cheng, S., Wang, Y.B., Song, L., Wang, S.L., Liu, J.Y., Wang, X.R., 2007. Effects of trichlorfon on progesterone production in cultured human granulosa–lutein cells. Toxicol. in Vitro 21, 912–918.

Karp, G., 2006. Cell and Molecular Biology: Concepts and Experiments, fourth ed. John Wiley & Sons, New York.

Kasibhatla, S., Amarante-Mendes, G.P., Finucane, D., Brunner, T., Bossy-Wetzel, E., Green, D.R., 1998. Acridine Orange/Ethidium Bromide (AO/EB) Staining to Detect Apoptosis. Cold Spring Harbor, New York (Chapter 15).

Kobayashia, D., Ahmed, S., Ishida, M., Kasai, S., Kikuchi, H., 2009. Calcium/calmodulin signaling elicits release of cytochrome c during 2,3,7,8-tetrachlorodibenzo-p-dioxin-induced apoptosis in the human lymphoblastic T-cell line, L-MAT. Toxicology 258, 25–32.

Li, P., Nijhawan, D., Budihardjo, I., Srinivasula, S.M., Ahmad, M., Alnemri, E.S., Wang, X., 1997. Cytochrome c and dATP-dependent formation of Apaf-1/caspase-9 complex initiates an apoptotic protease cascade. Cell 91, 479–489.

Li, Q., Minami, M., Hanaoka, T., Yamamura, Y., 1999. Acute immunotoxicity of p-chloronitrobenzene in mice. II. Effect of p-chloronitrobenzene on the immunophenotype of murine splenocytes determined by flow cytometry. Toxicology 137, 35–45.

Li, Q., Kobayashi, M., Kawada, T., 2007. Organophosphorus pesticides induce apoptosis in human NK cells. Toxicology 239, 89–95.

Lopes, R.B., Paraiba, L.C., Ceccarelli, P.S., Tornisielo, V.L., 2006. Bioconcentration of trichlorfon insecticide in pacu (*Piaractus mesopotamicus*). Chemosphere 64, 56–62.

Nakadai, A., Li, Q., Kawada, T., 2006. Chlorpyrifos induces apoptosis in human monocyte cell line U937. Toxicology 224, 202–209.

Ohkawa, H., Ohishi, N., Tagi, K., 1979. Assay for lipid peroxides in animal tissues by thiobarbituric acid reaction. Anal. Chem. 95, 351–358.

Ott, M., Gogvadze, V., Orrenius, S., Zhivotovsky, B., 2007. Mitochondria, oxidative stress and cell death. Apoptosis 12, 913–922.

Porter, A.G., Janicke, R.U., 1999. Emerging roles of caspase-3 in apoptosis. Cell. Death. Differ. 6, 99–104.

Pirnia, F., Schneider, E., Betticher, D.C., Borner, M.M., 2002. Mitomycin C induces apoptosis and caspase-8 and -9 processing through a caspase-3 and Fas-independent pathway. Cell Death Differ. 9 (9), 5–14.

Rea-Boutrois, A., Pontini, G., Greenland, T., Mehlen, P., Chebloune, Y., Verdier, G., Legras-Lachuer, C., 2008. Caprine arthritis–encephalitis virus induces apoptosis in infected cells in vitro through the intrinsic pathway. Virology 375, 452–463.

Roos, D.H., Puntel, R.L., Santos, M.M., Souza, D.O.G., Farina, M., Nogueira, C.W., Aschner, M., Burger, M.E., Barbosa, N.B.V., Rocha, J.B.T., 2009. Guanosine and synthetic organoselenium compounds modulate methylmercury-induced oxidative stress in rat brain cortical slices: involvement of oxidative stress and glutamatergic system. Toxicol. in Vitro 23, 302–307.

Saleh, A.M., Vijayasarathy, C., Masoud, L., Kumar, L., Shahin, A., Kambal, A., 2003. Paraoxon induces apoptosis in EL4 cell via activation of mitochondrial pathways. Toxicol. Appl. Pharmacol. 190, 47–57.

Saulsbury, M.D., Heyliger, S.O., Wang, K., Round, D., 2008. Characterization of chlorpyrifos-induced apoptosis in placental cells. Toxicology 244, 98–110.

Saulsbury, M.D., Heyliger, S.O., Wang, K., Round, D., 2009. Chlorpyrifos induces oxidative stress in oligodendrocyte progenitor cells. Toxicology 259 (1–2), 1–9.

Shi, H., Hudson, L.G., Liu, K.J., 2004. Oxidative stress and apoptosis in metal ion-induced carcinogenesis. Free Radical Biol. Med. 37, 582–593.

Soumis, N., Lucotte, M., Sampaio, D., Almeida, D.C., Giroux, D., Morais, S., Pichet, P., 2003. Presence of organophosphate insecticides in fish of the Amazon river. Acta Amazon 33, 325–338.

Susin, S.A., Daugas, E., Ravagnan, L., Samejima, K., Zamzami, N., Loeffler, M., Costantini, P., Ferri, K.F., Trinopoulou, T., Prévost, M.C., Brothers, G., Mak, T.W., Penninger, J., Earnshaw, W.C., Kroemer, G., 2000. Two distinct pathways leading to nuclear apoptosis. J. Exp. Med. 192, 571–580.

Wang, P., Chen, L.L., Yan, H., Li, J.C., 2008. Trichosanthin suppresses HeLa cell proliferation through inhibition of the PKC/MAPK signaling pathway. Cell Biol. Toxicol.. doi:10.1007/s10565-008-9102-x.

Yoshimura, K., Tanimoto, A., Abe, T., Ogawa, M., Yutsudo, T., Kashimura, M., 2002. Shiga toxin 1and 2 induce apoptosis in the amniotic cell line WISH. J. Soc. Gynecol. Invest. (1), 22–26.

Yu, F., Wang, Z., Ju, B., Wang, Y.Q., Wang, J., Bai, D., 2008. Apoptotic effect of organophosphorus insecticide chlorpyrifos on mouse retina in vivo via oxidative stress and protection of combination of vitamins C and E. Exp. Toxicol. Pathol. 59, 415–423.

Zhang, Y.M., Bhavnani, B.R., 2005. Glutamate-induced apoptosis in primary cortical neurons is inhibited by equine estrogens via down-regulation of caspase-3 and prevention of mitochondrial cytochrome c release. BMC Neurosci. 6 (2), 13–17.